Preferential Attachment of Membrane Glycoproteins to the Cytoskeleton at the Leading Edge of Lamella

Dennis F. Kucik,‡ Scot C. Kuo,* Elliot L. Elson,‡ and Michael P. Sheetz*

*Department of Cell Biology and Physiology, Department of Cell Biology, Duke University Medical Center, Durham, North Carolina 27710; and ‡Department of Biochemistry and Molecular Biophysics, Division of Biology and Biomedical Sciences, Washington University School of Medicine, St. Louis, Missouri 63110

Abstract. The active forward movement of cells is often associated with the rearward transport of particles over the surfaces of their lamellae. Unlike the rest of the lamella, we found that the leading edge (within 0.5 microns of the cell boundary) is specialized for rearward transport of membrane-bound particles, such as Con A–coated latex microspheres. Using a single-beam optical gradient trap (optical tweezers) to apply restraining forces to particles, we can capture, move and release particles at will. When first bound on the central lamellar surface, Con A–coated particles would diffuse randomly; when such bound particles were brought to the leading edge of the lamella with the optical tweezers, they were often transported rearward. As in our previous studies, particle transport occurred with a concurrent decrease in apparent diffusion coefficient, consistent with attachment to the cytoskeleton. For particles at the leading edge of the lamella, weak attachment to the cytoskeleton and transport occurred with a half-time of 3 s; equivalent particles elsewhere on the lamella showed no detectable attachment when monitored for several minutes. Particles held on the cell surface by the laser trap attached more strongly to the cytoskeleton with time. These particles could escape a trapping force of 0.7×10^{-6} dyne after 18 ± 14 (sd) s at the leading edge, and after 64 ± 34 (SD) s elsewhere on the lamella. Fluorescent succinylated Con A staining showed no corresponding concentration of general glycoproteins at the leading edge, but cytochalasin D–resistant filamentous actin was found at the leading edge. Our results have implications for cell motility: if the forces used for rearward particle transport were applied to a rigid substratum, cells would move forward. Such a mechanism would be most efficient if the leading edge of the cell contained preferential sites for attachment and transport.

REARWARD transport of surface-bound particles on locomoting cells is a well known phenomenon (Abercrombie et al., 1970; Dembo and Harris, 1981; Bray, 1970). When motile cells encounter particles seeded onto their substratum, cells pick up the particles and transport them centripetally over their dorsal surfaces. This rearward transport is exhibited only by cells capable of locomotion. After a few days in culture, fibroblasts cease locomotion and assume a polygonal shape; concurrently, transport of surface particles also ceases (Trinkaus, 1984). Although early investigators interpreted this particle transport as reflecting a rearward flow of the membrane (Abercrombie et al., 1970; Bray, 1970), evidence has been accumulating that particle transport is a cytoskeletal phenomenon. The plasma membrane moves forward passively with the locomoting cells, as was determined both by tracking diffusive beads (Kucik et al., 1990) and by photobleaching lipid probes (Lee et al., 1990). Rearward transport of some surface proteins trace the path of submembranous actin arcs (Heath, 1983), and polystyrene beads on the surface of fibroblasts are transported rearward at the same velocity as many cytoskeletal components (Fisher et al., 1988). Cell migration requires adherence to the substratum and the concomitant exertion of force upon it. Examination of the process by which the cytoskeleton attaches to and exerts force on adhered surface sites, such as the beads used in our studies, could provide insight into cell migration.

To examine particle transport, we used a single-beam optical gradient trap, also called laser tweezers or optical tweezers, both to place beads at various locations on the cell and to restrain bead movement. Radiation pressure from a focused laser beam can move particles ranging in size from hundreds of Angstroms to tens of micrometers (Ashkin et al., 1986, 1987*a*). If an infrared laser is used, the intensity levels required for controlling particle positions produce negligible damage in living cells. Living bacteria and yeast cells have been held in a laser trap for 5 h without apparent damage, even reproducing while trapped (Ashkin et al., 1987*a*).

In this study, we used the laser optical trap to move Con A–coated beads bound to membrane glycoproteins on the lamella of fish epidermal keratocytes. Fish epidermal keratocytes are ideal for this study because they have a uniform shape and a broad, rapidly moving lamella (Euteneuer and Schliwa, 1984; Cooper and Schliwa, 1985). The lack of

localized features within the lamella allows easy, unambiguous interpretation of bead movements (Kucik et al., 1989, 1990). We have observed two functionally different domains of the lamella: (*a*) the leading edge and the strip of membrane within 0.5 μm of the leading edge; and (*b*) the remainder of the lamella. Using membrane-bound beads, we show here that the leading edge of the lamella appears specialized for linking membrane proteins to a cytoskeletal-dependent transport system. We measure the initial kinetics of linking membrane-bound beads to this transport system and also show that the strength of such attachment can increase with time. In our studies, binding of Con A–coated beads to membrane glycoproteins appears irreversible and all subsequent particle movements are in the plane of the membrane. By restricting our analysis to beads already bound to membrane glycoproteins, we have focused on the cytoskeletal interactions of the bead-bound membrane glycoproteins, rather than changes in bead interactions with glycoproteins.

Materials and Methods

Cell Culture

Scales from goldfish (*Carassius auratus*) were placed in a drop of Amphibian Culture Medium (Gibco Laboratories, Grand Island, NY) on an acid-washed 22 × 22 mm #0 coverslip and covered with a second coverslip. Each pair of coverslips was held in a 35-mm cell culture dish. After 40 min, another 1 ml of Amphibian Culture Medium was added to each dish. Fish epidermal keratocytes were allowed to crawl from the scale onto one of the coverslips overnight.

Bead Preparation

A solution of 2 mg/ml Con A was prepared in 1 ml fish Ringer (Cooper and Schliwa, 1985). Either 0.5 ml of 40-nm gold bead suspension (Janssen Life Sciences Products, Piscataway, NJ) or 0.1 ml of 550-nm carboxylated latex beads (Polysciences, Inc., Warrington, PA) was added to this solution and incubated on ice for 30 min. Beads were washed with 5 mg/ml BSA in fish Ringer by centrifugation at 15,000 rpm in an Eppendorf centrifuge (Brinkmann Instruments Inc., Westbury, NY) at 4°C (30 min) and bath sonication of the pellet and resuspension in 5 mg/ml BSA. Beads were washed once more just before use.

Video Microscopy

Cells were mounted in viewing chambers (Schnapp, 1986) consisting of an aluminum coverslip holder, a 24 × 60 mm #0 coverslip, and the 22 × 22 mm #0 coverslip on which the cells had been grown. Stage medium consisted of fish Ringer with appropriate amounts of Con A–coated beads. Cells were observed by video-enhanced differential interference contrast microscopy on a microscope (IM-35; Zeiss, Oberkochen, Germany) (Schnapp, 1986). Images were collected with a camera (model 70; Dage-MTI Inc., Wabash, MI) and stored on s-VHS videotape. Images were digitized from the videotape for analysis. Positions of selected particles in the digitized images were determined automatically by computer and image processor for each video frame usually by the method of Gelles et al. (1988). In some cases, however, the centroid of the bright portion of the DIC image of the bead was calculated without cross-correlation analysis. Particle tracks were analyzed to compute diffusion coefficients and the velocity of directed movement as described previously (Sheetz et al., 1989).

Rhodamine Phalloidin Labeling

Cells were incubated at room temperature in fish Ringer with or without 1 μg/ml cytochalasin D for 20 min. Cultures were then rinsed twice with fish Ringer and fixed by incubation in 2% paraformaldehyde in fish Ringer at room temperature for 30 min, washed three times with fish Ringer, followed by extraction in −20°C acetone for 5 min and subsequently air dried. Cells were stained in 0.3 μg/ml rhodamine (TRITC) phalloidin (Sigma Chemical Co., St. Louis, MO) in 140 mM NaCl 10 mM phosphate, pH 7.4, (PBS) for 30 min at room temperature. Cultures were then rinsed twice with PBS and mounted on slides for fluorescence microscopy with 2% n-propylgallate in 50% glycerol.

FITC-sCon A Labeling

Cultures were fixed in 2% paraformaldehyde in fish Ringer for 30 min and washed three times with 5-min incubations in fish Ringer. Cells were stained for 10 min with 100 μg/ml FITC-succinylated Con A (FITC-sCon A)[1] (Sigma Chemical Co.) in 1 mg/ml cytochrome C in fish Ringer. Cultures were washed twice with fish Ringer and mounted for fluorescence microscopy as described above.

Construction and Calibration of the Laser Optical Trap

Details of the construction of our optical trap on the video-enhanced DIC microscope have been described elsewhere (Kuo et al., 1991) and are similar to the inverted design outlined in Block (1990). As shown in Fig. 1, the polarized beam from a 1 W TEM_{00}-mode near-infrared laser (wavelength 1.064 μm) (model C-95; CVI Corporation, Albuquerque, NM) was expanded with a 3× beam expander (CVI Corporation) and focused with an 80-mm focal length achromat lens (Melles Griot, Irvine, CA) into the epifluorescence port of a Zeiss IM-35 inverted microscope, which retained the converging relay lens of the epifluorescence port. A heat-reflecting dichroic mirror (Melles Griot) directed the beam onto the sample through the objective Wollaston prism and through the high numerical aperture Plan-Apo objective lens from Zeiss (63× 1.4 NA). The DIC analyzer was placed outside the path of the infrared beam to reduce unwanted polarization effects. The maximum particle retention force of the laser optical trap was calibrated using viscous drag, similar to methods described by Ashkin et al. (1986) and Block et al. (1989). Latex spheres were held against the flow of aqueous solutions pumped through a flow cell (Berg and Block, 1984) that exhibits laminar flow in the area of observation. The force of viscous drag (F) is approximated by Stokes law for a sphere: $F = 6 \pi \eta r \nu$ where r is the radius of the sphere, ν velocity of fluid flow, and η the viscosity of the medium. Calibrations were performed 3 to 5 μm (6–10 bead diameters) above the coverslip, where wall effects are <5%. The fluid viscosity was determined using an Ostwald viscometer. Using video microscopy, the local fluid velocity around the trapped sphere was determined by tracking either latex spheres which were unaffected by the laser trap and were moving with the fluid flow, or the trapped sphere after it slipped out of the influence of the laser trap (>1.5 μm from the center of the trap). The limiting velocity at which beads were retained in the optical trap indicated the maximum force which the trap could exert. Both water and dilute Ficoll 400 solutions (a Newtonian fluid) (Berg and Turner, 1979) were used, indicating a maximum retention force of 0.7×10^{-6} dyne (directed parallel to the substrate surface) for 550-nm latex spheres in the optical trap.

Results

Assay for Attachment of Con A–Coated Beads to the Cytoskeleton

Con A–coated 550-nm latex beads displayed two distinct behaviors when bound to the lamella of locomoting fish epidermal keratocytes: random diffusion and rearward transport. These two behaviors were previously reported and can be discriminated both qualitatively and quantitatively (see Sheetz et al., 1989; and Kucik et al., 1990). Qualitatively, particles undergoing directed transport appeared more restricted in mobility while experiencing net displacement (Fig. 2). Numerically, this difference is confirmed by the apparent diffusion coefficient: diffusing beads exhibited apparent diffusion coefficients ($3.1 \pm 1.4 \times 10^{-10}$ cm^2 sec^{-1} [SD]) an order of magnitude greater than that of transported beads

1. *Abbreviation used in this paper*: sCon A, succinylated Con A.

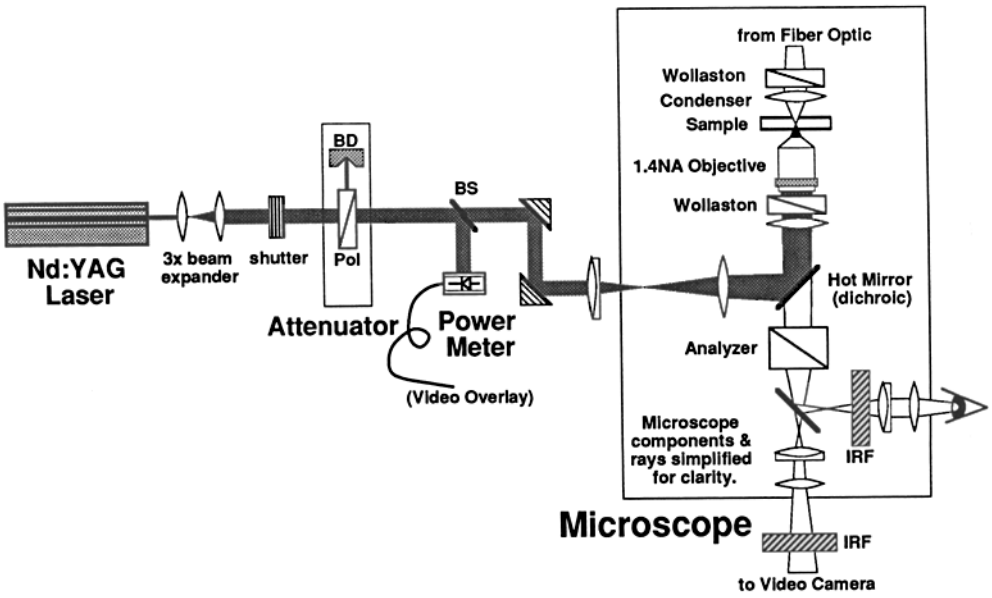

Figure 1. Construction of the Optical Trap. Detailed description is in Material and Methods. *BD*, beam dump; *BS*, beam splitter; *Pol*, polarizer; *IRF*, infrared filter.

($2.7 \pm 1.1 \times 10^{-11}$ cm^2 sec^{-1} [sd]). Quantitatively, in the frame of reference of the moving cell, the mean-squared displacement was linearly dependent upon the time interval for the diffusing particles whereas it was best fit by a quadratic dependence for the transported beads (see Sheetz et al., 1989). The average rate of displacement of the transported beads was 0.35 ± 0.15 (sd) μm/s and 0.08 ± 0.03 (sd) μm/s in a rearward direction relative to the cell edge and to the substratum, respectively (see note added in proof); whereas that of the diffusing beads was 0.0 ± 0.006 (sd) μm/s relative to the cell edge and 0.27 ± 0.12 (sd) μm/s forward relative to the substratum. Thus, the 550-nm Con A–coated particles exhibited diffusion behaviors similar to that described previously (Kucik et al., 1990).

Location of Particle Attachment to the Cytoskeleton

We observed that when Con A–coated beads were added to a culture of crawling cells, the beads encountered by the leading edge behaved differently from those that landed elsewhere on the lamella. When the cell's leading edge encountered particles on the glass surface, they were picked up and transported rearward (49 out of 51). In contrast, particles that settled out of the medium onto the surface of the lamella behind the leading edge diffused randomly in the plane of the membrane (10 out of 10). This observation suggested that the ability of particles to attach to the cytoskeleton was dramatically enhanced at the leading edge compared to the remainder of the surface of the lamella. However, the direct binding of beads in the medium to the lamellar surface was rare.

Placement of Beads at Specific Locations by the Laser Optical Trap

To investigate further the domain dependence of the process of attachment to the cytoskeleton, we used an infrared laser trap to place beads at various locations on the dorsal surface of locomoting cells. The single-beam optical gradient trap has previously been used to move or hold small particles (e.g., Ashkin et al., 1986, 1987*a*; Ashkin and Dziedzic, 1987*b*, 1989) and, at sufficiently high irradiation intensities, can distort unsupported membranes directly (Ashkin and Dziedzic, 1989). For fish epidermal keratocytes, our laser trap produced no measurable distortion of the keratocyte plasma membrane, even when the full laser power ($\sim 0.7 \times 10^{-6}$ dyne) was used to pull latex beads bound to the membrane.

As an indication that the intense laser light did not adversely affect cell behavior, we compared the behavior of beads seeded and released by the laser trap with the behavior of beads and cells that were never influenced by the laser. Beads held by the laser trap against the glass in the path of the cell were picked up by the cell and transported rearward (8 out of 8) with a concomitantly small diffusion coefficient. In contrast, those placed on the lamella behind the leading edge diffused randomly (80 out of 80) (Fig. 2 *B*) on the surface. If monitored for as long as 2 min (5 beads), none of these diffusing beads attached to the cytoskeleton. These data were consistent with our previous observations of beads which spontaneously settled out of the medium. Furthermore, >10 min irradiation with the laser trap did not change the velocity of cell movement. Thus, the laser trap introduced minimal perturbations to the behavior of cells and the attachment of Con A–coated beads to the cytoskeleton.

Binding of Beads to the Surface with the Optical Trap

When beads were brought to the lamellar surface and held there, the binding was not instantaneous. If the trap was turned off after only 1–2 s, about half of the particles released from the membrane and diffused away. This is consistent with our observation that beads freely diffusing in the medium would make many apparent contacts with the lamellar surface before binding. For the remaining studies the beads were held at the lamellar surface in the trap for 5–7 s, which assured that they would remain bound when the trap was turned off. Once bound to the lamella the beads could not be pulled off with the laser trap and, as stated above, there

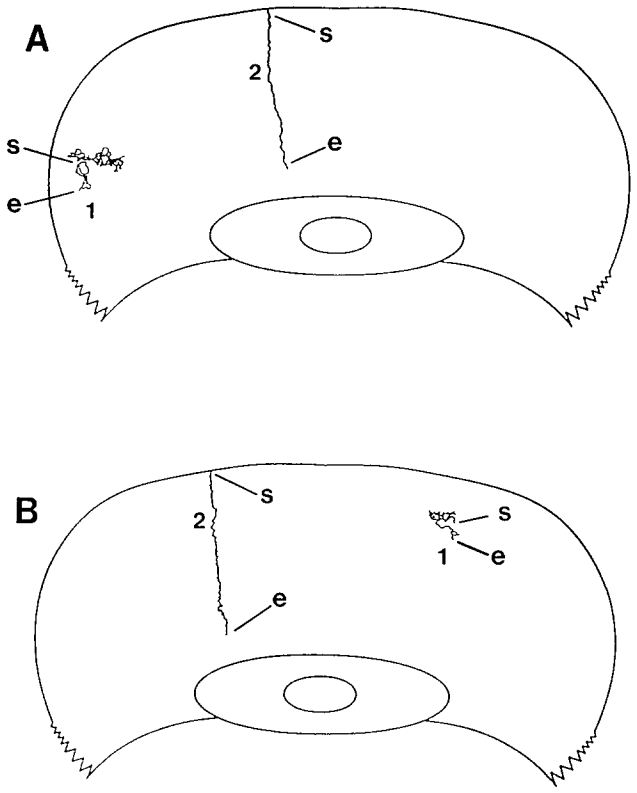

Figure 2. (*A*) Diffusing beads are easily distinguished from those undergoing rearward transport. Bead motion was monitored using video-enhanced DIC microscopy and recorded on videotape. Using nanometer-level tracking algorithms (Gelles et al., 1988, or similar procedures; see text) the bead position was determined for each video frame to generate bead trajectories. Each bead shown was tracked for 15 s, the trajectory was numerically compensated for cell translocation (Kucik et al., 1990), and the trajectories are drawn on the outline of a typical fish epidermal keratocyte. Bead *1* is diffusing randomly, while bead *2* is undergoing rearward transport. Arrows indicate starting and ending points. Quantitative analysis of these trajectories (Sheetz et al., 1989; Kucik et al., 1989) shows that the trajectory of bead *1* is consistent with a random walk ($p > 0.5$) while that of bead *2* is not ($p < 0.001$). Further, the random component of trajectory *2* corresponds to a diffusion coefficient of 9×10^{-12} cm^2/s, nearly two orders of magnitude lower than that of bead *1* ($D = 6 \times 10^{-10}$ cm^2/s). This disparity in the thermal motion of identical beads suggests that bead *2* is attached to a large, relatively immobile structure such as the cytoskeleton. (*B*) Manipulation with a laser trap does not change the behavior of Con A–coated beads. Con A–coated beads identical to those above were plucked from the medium and either held in the path of the cell (*1*) or placed directly on the lamella behind the leading edge (*2*). Bead *2* was picked up and transported, while bead *1* diffused randomly (see above for criteria by which random diffusion and systematic transport were assessed).

was no apparent distortion of the cell membrane in such attempts.

For the experiments described in the next section, a consistent protocol was used to bind beads to cells. Beads were plucked from the medium with the laser trap and held against the dorsal surface of the lamella (at least 2 μm inside of the cell edge) for 5–7 s before release. As described above, these beads diffused randomly over the membrane plane when released from the trap. These beads were allowed to diffuse for 30 s on the cell surface before further relocation by the laser. As presented later in the Discussion, this incubation should be sufficient for the bead's contact area to achieve steady-state saturation of the Con A–binding sites.

Attachment of Bound Beads to the Cytoskeleton

The laser trap allowed us to determine the domain preference for attachment of bound beads to the cytoskeleton. A diffusing, but cell-bound bead (bound by the protocol described above) could be recaptured by the laser trap and dragged along the plane of the membrane to the leading edge of the cell. After a few seconds of restraint to within 0.5 μm of the apparent edge, the bead would make initial movements toward the rear of the cell at normal velocities of rearward transport. In most cases, the bead would not completely escape but would rapidly spring back (<67 ms) to the center of the laser trap (example in Fig. 3). When the trap was turned off, however, these beads were likely to be transported rearward.

The time dependence of attachment to the transport system was measured using the laser trap. Beads originally bound elsewhere on the lamella were held by the laser at the front edge of cells for various time intervals. Upon release from the laser trap, beads were characterized as undergoing random diffusion or directed transport. For each time interval, the fraction of trials which showed bead transport yielded the probability that the bead had become attached to the transport machinery in that interval. For short times, the probability of transport varied exponentially with time (Fig. 4), with a time constant of 0.36 s^{-1}, and reached an apparent limiting value of 80% of the particles undergoing transport in 10 s. This experiment records any bead attachment to the cytoskeleton and consequent transport, as long as that attachment is strong enough to resist the forces generating Brownian movements.

When held continuously at the leading edge for times longer than 10 s, stronger particle attachment can be observed. When the laser was used to continuously restrain 550-nm beads with a maximum of 0.7×10^{-6} dyne trapping

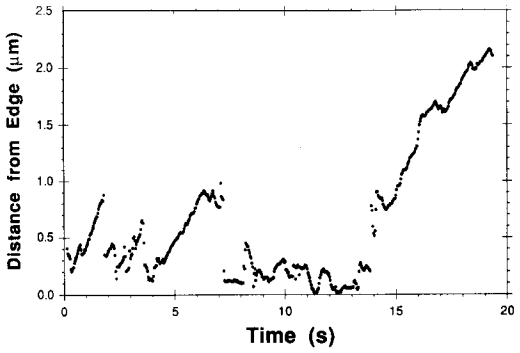

Figure 3. Position of bead restrained near the leading edge. Using the laser trap, a 550-nm Con A–coated bead was bound to the lamella 3 μm behind the leading edge, as described in the text. After 30 s of free diffusion to confirm that the bead was bound to the cell surface, the bead was moved (at time t = 0) and restrained within 0.5 μm of the leading edge of the cell using the full laser power (0.7×10^{-6} dyne). The perpendicular distance of the bead from the leading edge is plotted as a function of time from initial restraint at the leading edge.

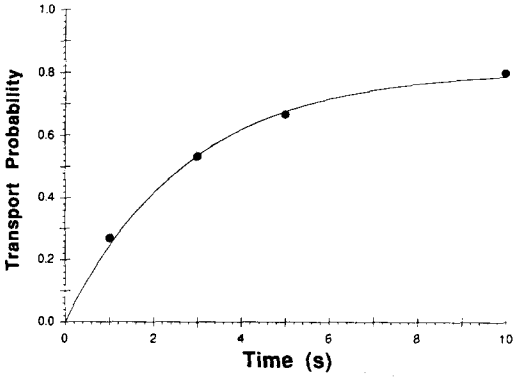

Figure 4. Probability of attachment of beads to the transport mechanism as a function of time held at the leading edge. Beds were held for the specified time and then released to determine attachment to the transport mechanism. 60 separate trials were performed in this experiment (15 at each time point), and the probability of successful attachment was measured as described in the text. Nonlinear least squares curve-fitting with a single exponential yields a time constant of 0.36 s^{-1} and apparent maximal probability of 81%. The same curve is generated from a model of reversible attachment with 0.29 s^{-1} and 0.068 s^{-1} for on and off rates, respectively.

force, beads, which made early unsuccessful attempts at escaping the trap, would often succeed in escaping at later times (Figs. 3 and 5). At the leading edge of the lamella, these stronger attachments and transport took much longer to form than the weaker attachments of the previous experiment (for the former, an average of 18 ± 14(sd) s; for the later, a half-time of 3 s). Although particles diffusing randomly over the body of the lamella rarely attached to the transport system, we found that holding beads stationary (with respect to the cell) with the laser trap promoted rearward transport, with an average time of escape of 64 ± 34(sd) s for those particles that were transported (Fig. 5). Strong attachment of beads to the cytoskeleton occurred much more rapidly at the leading edge than over the rest of the lamella.

Size Dependence of Attachment

The attachment of externally bound particles to the cytoskeleton via membrane proteins was highly dependent upon particle size. We observed that Con A–coated 0.19 μm latex particles attached to the cytoskeleton only when held at the leading edge for more than 10 s (10 trials; the weaker force of the trap on the smaller particles made these experiments difficult). Furthermore, aggregates (>100 nm) of 40-nm gold particles were transported rearward, but single gold particles were very rarely transported. Over 1,000 single gold particles were followed for over 2 min each with only three transport events observed. Thus, the probability of attachment to the cytoskeleton and concomitant transport increases with the size of the particle.

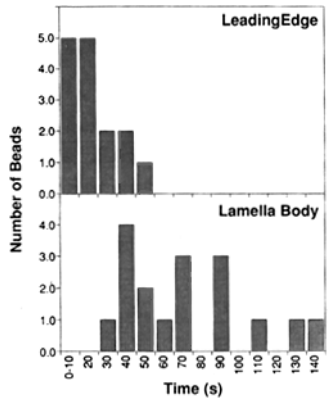

Figure 5. Time required for the cell to pull a bead out of the laser trap. (*Top*) Beads held at the leading edge. (*Bottom*) Beads held behind the leading edge on the body of the lamella. On average, beads held at the leading edge were pulled out of the trap much more quickly than those held behind the leading edge.

Behavior of Particles after Cytoskeletal Transport

Once beads became attached, they tended to stay on the cytoskeletal "conveyor" until they crossed the lamella and reached the endoplasm region over the cell body. Occasionally (two of over 200 beads followed), a bead would detach and resume Brownian movement while still on the lamella. However, all beads which reached the vesicle-rich endoplasm ceased directed motion and began random diffusion. During our experiments, we did not observe endocytosis of beads.

Although these beads regained diffusive behavior over the endoplasm, they were different from diffusive beads bound to the lamella. "Experienced" beads diffusing over the endoplasm were difficult to drag back to the front of the cell a second time. Frequently in such attempts, beads were pulled from the grip of the laser and transported rearward again while still in the mid-lamella area (data not shown). In contrast, beads diffusing randomly on the dorsal surface of the lamella could be trapped and moved to various locations on the lamella without difficulty. Experiments addressing the differences between these two classes of diffusing bead complexes were beyond the scope of this study.

Structural Specialization at the Leading Edge

To explore possible structural correlations with the specialization of the leading edge for particle transport, we examined the distribution of cytoskeleton and Con A–binding sites. The actin at the leading edge of nerve growth cones is more resistant to cytochalasins B and D than the actin in the rest of the cell (Forscher and Smith, 1988). Although actively migrating fish epidermal keratocytes tended to round up and detach from the substrate when treated with cytochalasin, cells which were spreading rather than translocating remained spread in the presence of cytochalasin (data not shown). As with other types of spreading cells stained with TRITC–phalloidin, the actin filaments at the leading edge of fish keratocytes were resistant to cytochalasin D (Fig. 6 *F*). Unlike the actin filaments, fluoresceinated succinylated Con A appeared uniformly distributed over the edge and the body of the lamella (Fig. 6 *B*). We did not observe an enhanced concentration of Con A–labeled membrane glycoproteins to match the regional specialization of actin filaments at the leading edge of the lamella.

Discussion

We have found that the leading edge of locomoting fish epidermal keratocytes is specialized for attachment of Con A–coated beads to a centripetal transport system. Weak attachment of particles occurs much more rapidly at the leading edge compared to the rest of the lamella. Formation of stronger attachments, as determined by particle escape from the laser trap, is also more rapid at the leading edge than the

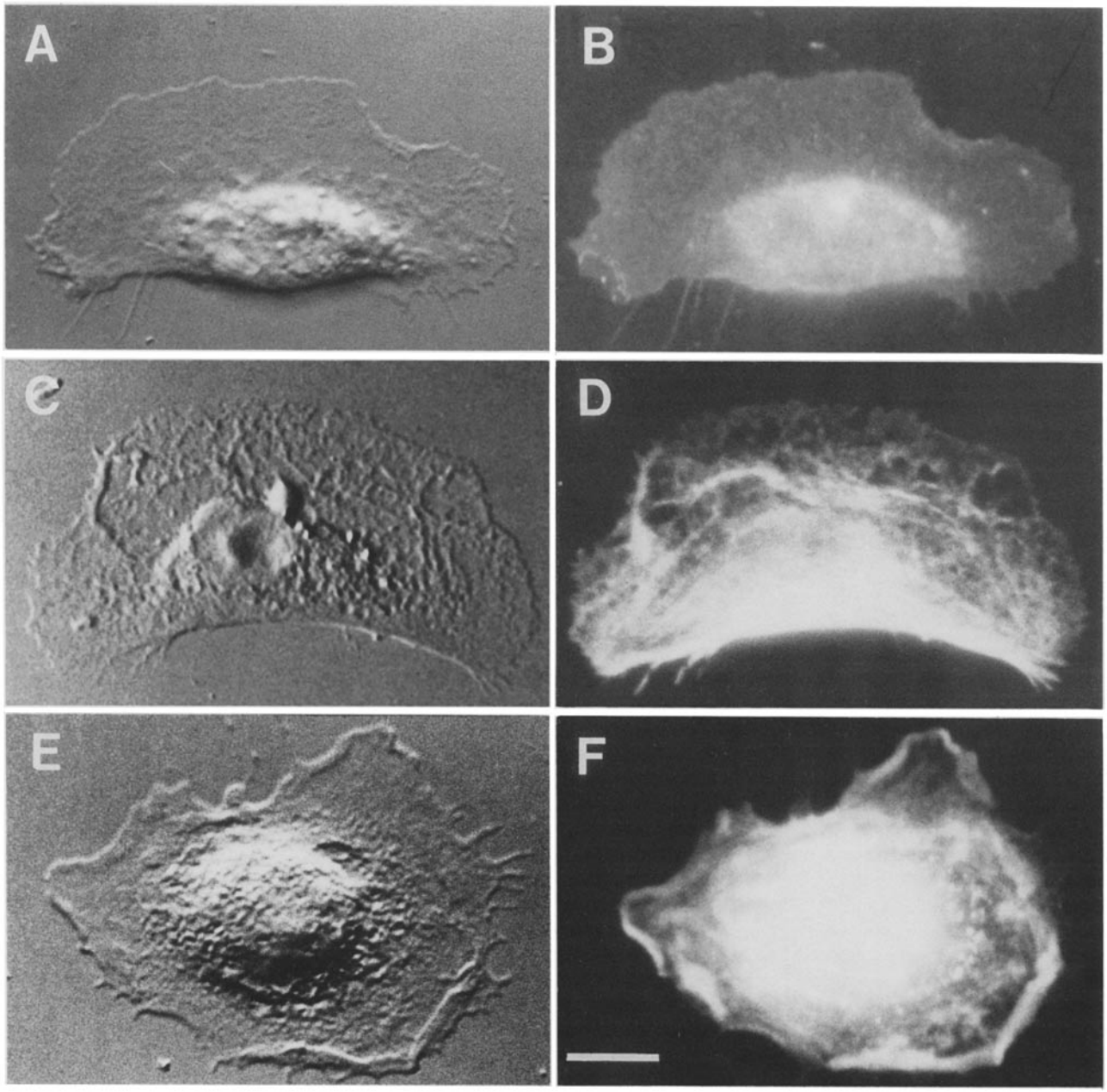

Figure 6. Micrographs of the distribution of fluorescent Con A (*B*) and actin filaments (*D* and *F*) as well as the corresponding cell morphology (*A*, *C*, and *E*) of keratocytes. Cells were fixed in 2% paraformaldehyde prior to labeling with FITC-sConA (*A* and *B*) or rhodamine phalloidin (*C–F*). The sCon A binding was found to be uniform over the lamella with no apparent excess concentration at the leading edge (*B*). Actin filaments were found concentrated at the leading edge in 1 μg/ml cytochalasin D–treated cells (*E* and *F*) whereas they were distributed throughout the lamella in moving cells (*C* and *D*) (c.f., Forscher and Smith, 1988). Bar, 10 μm.

remainder of the lamella. The reduced diffusion coefficient and systematic transport of the particles suggests that they were linked to actively moving components of the cytoskeleton. Much evidence exists for the rearward migration of the cytoskeleton in the lamella (Wang, 1985; Okabe and Hirokawa, 1989; and Forscher and Smith, 1988) and the cotransport of beads on the external surface (Fisher et al., 1988). Bead attachment to such cytoskeletal transport is clearly mediated by membrane components which are bound to and consequently cross-linked by the Con A–coated beads.

By following only beads already bound to membrane glycoproteins, the kinetics of particle transport preferentially reflects the kinetics of membrane glycoprotein attachment and transport. In our experiments, we allowed bound beads to diffuse on the membrane for over 30 s before being moved to the leading edge. Based on the concentration and rate of diffusion of membrane glycoproteins, this interval should be long enough for the Con A binding sites of the contact area of the bead to reach saturation with the glycoproteins (Bell, 1978). Release of bound glycoproteins is probably very slow

because of their strong association with Con A. Experimentally, even small (40-nm gold) Con A–coated particles rarely detached from cell surface glycoproteins. Overall, we expect that most of the membrane glycoproteins bound to a bead will move with it as the bead is moved to the leading edge.

Although we showed that the laser trap did not adversely affect cell behavior or bead transport, the trap did have a subtle influence on the attachment process. Beads held with the trap over the body of the lamella could attach to the cytoskeleton, with an average time to escape the trap of 64 s. Without the trap, the diffusing beads never attached to the cytoskeleton over equivalent times. Perhaps the mere restriction of bead movement allowed more efficient recruitment of transport factors, enhancing the rate of attachment and transport. However, we cannot rule out other explanations specific to the laser, such as localized heating because of the laser irradiation. The heating effect of the trap should only be a few degrees centigrade (Ashkin et al., 1987*a*; Block, 1990), but has not been measured directly. Such subtle effects of the laser do not affect the conclusion that the leading edge is specialized for attachment and transport.

Even though the initial kinetics of the attachment of beads to the cytoskeletal transport system at the leading edge appears to be a first-order reaction (rate constant of 0.36 s^{-1}), the overall process is likely to be more complex. Weak attachment and transport can be distinguished from the stronger transport linkages which appear with time. The initial, weaker linkages can dissociate from the transport system, and the laser trap makes those events more apparent since beads pop back into the trap. This process must be distinguished from measuring the force of the translocating motor, since we have not stalled moving particles. As discussed above, we believe that the membrane glycoprotein had detached from the transport machinery, rather than the bead detaching from the membrane protein. However, we cannot exclude the possibility that specific glycoproteins mediating particle transport detach from the bead, while other glycoproteins keep the bead bound to the membrane.

Stronger linkages appear to form with time at the leading edge. Several hypotheses could explain the nature of these stronger linkages: (*a*) although the weak linkages are supposed to dissociate rapidly, the stochastic nature of single-molecule events could allow a weak linkage to persist long enough for beads to escape the trap; (*b*) a strong linkage might consist of multiple weak linkages which form over time; or (*c*) strong and weak linkages might be entirely different with different kinetics of formation. Resolution of these alternatives is necessary to interpret the kinetics properly. Another complication for interpreting the kinetics is the lack of information about the mechanical nature of protein–protein linkages, particularly about the effect of restraining forces on the stability of these linkages.

Most transported beads, upon reaching the endoplasm region, resumed Brownian movement, consistent with a model in which actin filaments of the transported cytoskeleton are disassembled and then recycled. It has been proposed that the lamellipodial cytoskeleton is assembled at the leading edge and flows rearward as the cell moves (Wang, 1985; Bray and White, 1988). The site of disassembly of these actin filaments appears to be the transition zone between the lamella and the cell body. For example, when nerve growth cones are treated with cytochalasin B, actin assembly at the front edge stops. The filamentous actin present in the lamella then flows rearward, to disappear at this transition zone (Forscher and Smith, 1988). Even in untreated cells, this motion of the lamellipodial cytoplasm, composed almost exclusively of actin and actin binding proteins (Small, 1982), is visible by video-enhanced DIC microscopy as retrograde waves (Forscher et al., 1987). The waves originate at the leading edge and disappear at the transition zone. This motion is also similar to retrograde movement of ruffles, observed in fibroblasts and many other cell types, and to the process of capping of cross-linked surface glycoproteins in lymphocytes (reviewed in Bray and White, 1988). Actin disassembly in the transition zone may mediate the release of the Con A–coated beads (and their bound membrane glycoproteins) from the cytoskeleton and allow the beads to resume Brownian movement.

Correlating with our observation of a specialized particle transport function at the leading edge, there is much evidence that the cytoskeleton in this region of many cells is different. We have already mentioned the cytochalasin resistance of actin filaments at the leading edge of growth cones (Forscher and Smith, 1988), fibroblasts (Schwab and Elson, unpublished results), and fish keratocytes (Fig. 6 *F*). Myosin I is concentrated near the leading edge (Fukui et al., 1989) of amoeba, as are other actin-binding proteins in nerve growth cones (Letourneau and Shattuck, 1989). In contrast, evidence for corresponding specialization of membrane glycoproteins at the leading edge is less clear. Although there is evidence for the concentration of specific glycoproteins at the leading edge of neuronal growth cones (Sheetz et al., 1990), the apparent concentration of other glycoproteins at the leading edge resulted from increased amounts of membrane at the leading edge (Pytowski et al., 1990). Specifically, we found no concentration of Con A receptors corresponding to the transport specialization of the leading edge. However, bulk sCon A staining cannot resolve the concentration of a specific receptor subpopulation at the leading edge. Future studies with more specific ligands coating the beads would address cell surface specialization at the leading edge, as well as the propensity of specific receptors for rearward transport.

A specialized functional role of the leading edge of lamellipodia is suggested by this study. A mechanism by which a cell can attach cross-linked membrane proteins to the cytoskeleton and then exert rearward force on the resultant protein complex has obvious implications for the processes of cell migration and substrate recognition. If a similar attachment were made to an adhesion complex bound to the substratum, then rearward force on this site would result in forward motion of the cell. The most efficient forward movement would result if those attachments formed at the leading edge of the cell. Rapidly migrating cells, such as the fish keratocytes, might have the strongest coupling between the substratum and the cytoskeleton as it flows rearward in the cell. Slippage, or apparent rearward movement of the cytoskeleton relative to the substratum, could result from inefficient coupling of adhesion sites to the rearward moving cytoskeleton, or could result from portions of the cytoskeleton shearing from the lower layer attached to the substratum. Further studies will clarify the implications of our novel observation that the leading edge is enhanced for cytoskeletal attachment and transport.

We thank Hong Qian for helpful discussions.

Supported by National Institutes of Health grants NS23345 and GM36277 to M. P. Sheetz and GM38838 to E. L. Elson; and a Muscular Dystrophy Association grant to M. P. Sheetz. S. C. Kuo was supported by a grant from The Jane Coffin Childs Memorial Fund for Medical Research.

Received for publication 19 September 1991 and in revised form 15 May 1991.

Note Added in Proof: The immobility relative to the substratum of the beads linked to the cytoskeleton corresponds to the immobility of the lamellar actin cytoskeleton recently observed in locomoting fish epidermal keratocytes (J. A. Theriot and T. J. Mitchison. 1991. *Nature (Lond.)*. 352:126–131). Apparently surface particles and the cytoskeleton to which they are attached are fixed relative to the substratum as the bulk of the cell is drawn forward past them, presumably by cytoskeletal motors.

References

Abercrombie, M., J. E. M. Heaysman, and S. M. Pegrum. 1970. The locomotion of fibroblasts in culture III. Movements of particles on the dorsal surface of the leading lamella. *Exp. Cell Res.* 62:389–398.

Ashkin, A., J. Dziedzic, J. E. Bjorkholm, and S. Chu. 1986. Observation of a single-beam gradient force optical trap for dielectric particles. *Opt. Lett.* 11:288–290.

Ashkin, A., J. M. Dziedzic, and T. Yamane. 1987*a*. Optical trapping and manipulation of single cells using infrared-laser beams. *Nature (Lond.)*. 330:769–771.

Ashkin, A., and J. M. Dziedzic. 1987*b*. Optical trapping and manipulation of viruses and bacteria. *Science (Wash. DC)*. 235:1517–1520.

Ashkin, A., and J. M. Dziedzic. 1989. Internal cell manipulation using infrared laser traps. *Proc. Natl. Acad. Sci. USA*. 86:7914–7918.

Bell, G. I. 1978. Models for the specific adhesion of cells to cells. *Science (Wash. DC)*. 200:618–627.

Berg, H. C., and S. M. Block. 1984. A miniature flow cell designed for rapid exchange of media under high-power microscope objectives. *J. Gen. Microbiol.* 130:2915–2920.

Berg, H. C., and L. Turner. 1979. Movement of microorganisms in viscous environments. *Nature (Lond.)*. 278:349–351.

Block, S. M., D. F. Blair, and H. C. Berg. 1989. Compliance of bacterial flagella measured with optical tweezers. *Nature (Lond.)*. 338:514–518.

Block, S. M. 1990. Optical tweezers: a new tool for biophysics. *In* Noninvasive Techniques in Cell Biology. J. K. Foskett and S. Grinstein, editors. Wiley-Liss, Inc. New York. 375–402.

Bray, D. 1970. Surface movements during the growth of single explanted neurons. *Proc. Natl. Acad. Sci. USA*. 65:905–910.

Bray, D., and J. G. White. 1988. Cortical flow in animal cells. *Science (Wash. DC)*. 239:883–888.

Cooper, M. S., and M. Schliwa. 1985. Electrical and ionic controls of tissue cell locomotion in DC electric fields. *J. Neurosci. Res.* 13:223–244.

Dembo, M., and A. K. Harris. 1981. Motion of particles adhering to the leading lamella of crawling cells. *J. Cell Biol.* 91:528–536.

Euteneuer, U., and M. Schliwa. 1984. Persistent, directional motility of cells and cytoplasmic fragments in the absence of microtubules. *Nature (Lond.)*. 310:58–61.

Fisher, G. W., P. A. Conrad, R. L. DeBiasio, and D. L. Taylor. 1988. Centripetal transport of cytoplasm, actin, and the cell surface in lamellipodia of fibroblasts. *Cell Motil. and Cytoskeleton*. 11:235–247.

Forscher, P., and S. J. Smith. 1988. Actions of cytochalasins on the organization of actin filaments and microtubules in a neuronal growth cone. *J. Cell Biol.* 107:1505–1516.

Forscher, P., L. K. Kaczmarek, J. Buchanan, and S. J. Smith. 1987. Cyclic AMP induces changes in distribution and transport of organelles within growth cones of Aplysia bag cell neurons. *J. Neurosci.* 7:3600–3611.

Fukui, Y., T. J. Lynch, H. Brzeska, and E. D. Korn. 1989. Myosin I is located at the leading edges of locomoting Dictyostelium amoebae. *Nature (Lond.)*. 341:328–331.

Gelles, J., B. J. Schnapp, and M. P. Sheetz. 1988. Tracking kinesin-driven movements with nanometer-scale precision. *Nature (Lond.)*. 331:450–453.

Heath, J. P. 1983. Direct evidence for microfilament-mediated capping of surface receptors on crawling fibroblasts. *Nature (Lond.)*. 302:532–534.

Kucik, D. F., E. L. Elson, and M. P. Sheetz. 1989. Forward transport of glycoproteins on leading lamellipodia in locomoting cells. *Nature (Lond.)*. 340:315–317.

Kucik, D. F., E. L. Elson, and M. P. Sheetz. 1990. Cell migration does not produce membrane flow. *J. Cell Biol.* 111:1617–1622.

Kuo, S. C., J. Gelles, E. Steuer, and M. P. Sheetz. 1991. A model for kinesin movement from nanometer-level measurements of kinesin and cytoplasmic dynein and force measurements. *J. Musc. Res. & Cell Mot.* In press.

Lee, J., M. Gustafsson, K. E. Magnusson, and K. Jacobson. 1990. The direction of membrane flow in locomoting polymorphonuclear leukocytes. *Science (Wash. DC)*. 247:1229–1233.

Letourneau, P. C., and T. A. Shattuck. 1989. Distribution and possible interactions of actin-associated proteins and cell adhesion molecules of nerve growth cones. *Development*. 105:505–519.

Okabe, S., and N. Hirokawa. 1989. Incorporation and turnover of biotin-labeled actin microinjected into fibroblastic cells: an immunoelectron microscopic study. *J. Cell Biol.* 109:1581–1595.

Pytowski, B., F. R. Maxfield, and J. Michl. 1990. F_c and $C3_{bi}$ receptors and the differentiation antigen BH2-Ag are randomly distributed in the plasma membrane of locomoting neutrophils. *J. Cell Biol.* 110:661–668.

Schnapp, B. J. 1986. Viewing single microtubules by video light microscopy. *Meth. Enzymol.* 134:561–573.

Sheetz, M. P., S. Turney, H. Qian, and E. L. Elson. 1989. Nanometre-level analysis demonstrates that lipid flow does not drive membrane glycoprotein movements. *Nature (Lond.)*. 340:284–288.

Sheetz, M. P., N. L. Baumrind, D. S. Wayne, and A. L. Pearlman. 1990. Concentration of membrane antigens by forward transport and trapping in neuronal growth cones. *Cell*. 61:231–241.

Small, J. V. 1982. Organizations of actin and fibroblast locomotion. *In* Embryonic Development, Part B. Cellular Aspects. M. M. Burger and R. Wever, editors. Alan R. Liss, New York. 341–358.

Trinkaus, J. P. 1984. Prentice-Hall, Englewood Cliffs, NJ. Chapter 7.

Wang, Y. L. 1985. Exchange of actin subunits at the leading edge of living fibroblasts: possible role of treadmilling. *J. Cell Biol.* 101:597–602.